Journal of the Serbian Chemical Society
JSCS-info@shd.org.rs • www.shd.org.rs/JSCS

J. Serb. Chem. Soc. 85 (1) 37–51 (2020)
JSCS–5281

UDC 577.164.1+542.9+547.571'551:546.881.4–31:615.279
Original scientific paper

Oxovanadium(IV) complexes of the pyridoxal Schiff bases: Synthesis, experimental and theoretical characterizations, QTAIM analysis and antioxidant activity

PARISA GHORBANI[1], S. ALI BEYRAMABADI[2]*, MASOUD HOMAYOUNI-TABRIZI[3]** and PARICHEHREH YAGHMAEI[1]

[1]Department of Biology, Science and Research Branch, Islamic Azad University, Tehran, Iran, [2]Department of Chemistry, Mashhad Branch, Islamic Azad University, Mashhad, Iran and [3]Department of Biology, Mashhad Branch, Islamic Azad University, Mashhad, Iran

(Received 29 January, revised 14 April, accepted 24 May 2019)

Abstract: Two vanadyl complexes of the pyridoxal Schiff bases have been newly synthesized and characterized by several experimental methods, where the 4,4′-[1,4-butanediylbis-[(*E*)-nitrilomethylidyne])bis[5-hydroxy-6-methyl--3-pyridinemethanol] and *trans*-4,4′-[1,2-cyclohexanediylbis-[(*E*)-nitrilo-methylidyne]]bis[5-hydroxy-6-methyl-3-pyridinemethanol] Schiff base were used. Geometry optimization, assignment of the IR vibrational frequencies and the natural bond orbital (NBO) analysis of the complexes have been calculated by employing the density functional theory (DFT) approaches. Deprotonated form of the Schiff bases ($\mathbf{L}^{2-}$) acts as a tetradentate N_2O_2 ligand, which coordinates to the V(IV) *via* two phenolate oxygens and two imine nitrogens. In the square–pyramidal geometry of the [VO(**L**)], the apical position is occupied by an oxo ligand. The DFT-calculated vibrational frequencies show a good consistency with the corresponding experimental values, confirming suitability of the optimized geometries for the complexes. Characteristics of the bonding interactions have been explored using the quantum theory of atoms in molecule (QTAIM) analysis. The complex formation results in decrease in strength of the C–N bond of the azomethine group and increase in the strength of the C–O bonds of the phenolate group. High-energy gaps approve stability of the complexes. Both of the complexes show significant radical scavenging activities against the ABTS and DPPH radicals, even higher than the BHA.

Keywords: Schiff base; pyridoxal; DFT; oxovanadium; AIM; antioxidant.

*,** Corresponding authors. E-mail: (*)beiramabadi@yahoo.com, beiramabadi6285@mshdiau.ac.ir; (**)mmhomayouni6@gmail.com
https://doi.org/10.2298/JSC190129055G

INTRODUCTION

The Schiff bases and their complexes are of great importance in many areas especially in the biology with activities such as antibacterial,[1–3] antifungal,[2] antimicrobial,[4] antidiabetic[5] and anticancer.[6,7] Among them, the oxovanadium(IV) complexes of the Schiff bases exhibit beneficial catalytic[8,9] and biological activities such as the antimicrobial[3] and antidiabetic.[5,10]

3-hydroxy-5-(hydroxymethyl)-2-methylpyridine-4-carbaldehyde or pyridoxal is one form of Vitamin B_6,[11] which plays a cofactor role in many biosynthetic proceses such as the dehydration of serine and threonine, decarboxylation and racemization of amino acids and transamination.[12] Also, pyridoxal, necessary for growth of some beneficial bacteria, shows anticancer activity, too. The Schiff bases derived from the pyridoxal have been widely studied. Metal complexes of these Schiff bases show important biological applications as the antimicrobial,[13] antioxidant[14] and anticancer agents.[7,15] Among them, the vanadium complexes of pyridoxal Schiff bases display great biological activities such as the antioxidant,[16] antimicrobial[4,17] and insulin enhancing properties.[5] These prompt us to synthesize and characterize two new oxovanadium(IV) complexes of the pyridoxal Schiff bases. The employed Schiff bases were 4,4′-[1,4-butanediylbis-[(*E*)-nitrilomethylidyne])bis[5-hydroxy-6-methyl-3-pyridinemethanol] [=H_2A] and *trans*-4,4′-[1,2-cyclohexanediylbis-[(*E*)-nitrilo-methylidyne]]bis[5-hydroxy-6-methyl-3-pyridinemethanol] [=H_2B]. Previously, the synthesis and characterization of the H_2A and H_2B Schiff bases were reported in literature,[18,19] respectively. The synthesized V(IV) complexes have been characterized by several experimental methods. Geometry optimization, theoretical assignment of the IR spectra of the complexes and their NBO analysis have been done by employing the DFT methods. Another aim of this work was investigation on the bonding interactions by employing the QTAIM analysis.

EXPERIMENTAL

Material and methods

2,2-diphenyl-1-(2,4,6-trinitrophenyl)hydrazyl (DPPH) and 2,2′-azinobis(3-ethylbenzothiazoline-6-sulfonic acid (ABTS) were purchased from the Sigma-Aldrich Company. All of the other used chemicals were obtained from the Merck Company, and were employed without any further purification. The used Schiff bases were synthesized as reported previously, H_2A[18] and H_2B.[19] Melting points were obtained using an electrothermal 9100 melting point apparatus. The IR spectra were recorded on a Bruker Tensor 27 spectrophotometer from KBr disks. The mass spectra were obtained on a Shimadzu GC-MS QP 1100 EX, where the atmospheric pressure chemical ionization was used. A Heraeus elemental analyzer CHN-O-Rapid was used for the CHN elemental analysis. A Hitachi 2-2000 atomic absorption spectrophotometer was used for determination of percentage of V^{4+} in the complexes.

Synthesis of the complexes

For synthesis of each oxovanadium(IV) complex, 2 mmol of the corresponding Schiff base was dissolved in methanol (20 ml). Then, 4 mmol of the NEt_3 base was added to the

solution of the Schiff base ligand. The mixture was stirred for several minutes. A solution, of 2 mmol (0.506 g) of $VO(SO_4)\cdot 5H_2O$ in 10 ml methanol, was added dropwise to the Schiff base solution. The obtained mixture was stirred for 3 h at 40 °C. The precipitates were filtered off, washed with methanol and dried in an oven. [VO(A)] and [VO(B)] are dark-green and dark-khaki, respectively, yields of which were 76 and 71 %, respectively. They are decomposed at 280 and 203 °C, respectively.

DPPH assay

DPPH was dissolved in ethanol and its radical form obtained. DPPH has the highest absorbance at 517 nm. A 0.1 mM solution of DPPH was prepared in 95 % ethanol with a 1:1 volume ratio with each of the two investigated complexes or standard compound. The solution was placed in the dark for 30 min at 37 °C. The absorbance of the samples was then read at 517 nm. In order to compare the activity of the complexes, butylated hydroxyanisole (BHA) was used as a positive control. To determine the IC_{50} (the concentration required to inhibit 50 % antioxidant activity) for the investigated complexes and standard compound, DPPH assay was performed at five different concentrations (62.5–500 mg/mL) of the complex solution and standard compound. Each experiment was performed in three rounds and the mean values were calculated. The percentage of radical scavenging activity was calculated by the following equation: DPPH radical scavenging (%) = $100(A_{\text{Control}} - A_{\text{Sample}}/A_{\text{Control}})$

In this regard, A_{Control} represents the absorbance of the control solution, which contains 0.1 mM DPPH solution and distilled water instead of solution of the Schiff base complexes, and A_{Sample} indicates the absorbance of the sample solution of the [VO(A)] and [VO(B)] complexes.

ABTS assay

The ABTS molecule was used in this method. In order to prepare an ABTS radical solution, 2 mL of 7 mM ABTS and 1 mL of 2.45 mM potassium persulfate were mixed together for 16 hours in darkness at 25 °C. It was subsequently diluted with addition of water to obtain an absorbance of 0.70±0.02 at 734 nm. Then, the diluted ABTS radical solution was mixed in a 1:1 volume ratio with the [VO(A)] and [VO(B)] solutions at different concentrations (62.5––500 mg/mL). After incubation for 1 h in 37 °C, the absorbance of the solution was evaluated at 734 nm. This experiment was conducted to obtain the IC_{50} at five different concentrations of the [VO(A)] and [VO(B)] complexes and standard compound. The BHA was used as a standard compound. The control solution containded of distilled water instead of the complexes or standard solution. This experiment was performed in three rounds and the mean values were calculated. The percentage of radical scavenging activity was calculated by the following equation: ABTS radical scavenging (%) = $100(A_{\text{Control}} - A_{\text{Sample}}/A_{\text{Control}})$, where the A_{Control} and A_{Sample} represent absorbance of the control solution and the sample solution, respectively.

THEORETICAL METHODS

All of the DFT calculations were carried out with the B3LYP functional[20] as implemented in the Gaussian 03 program package.[21] The 6-311+G(d,p) basis set was employed except for the vanadium atom, where the LANL2DZ basis set[22] was used. For better results, the effective core potential functions of the LANL2DZ basis set was considered.

Geometries of two complexes have been optimized, which have no imaginary frequency, confirming suitability of the optimized geometries for the complexes. Structures were visualized by using the Chemcraft 1.7 program.[23] Frequency calculations were done on the optimized geometries to identify the IR spectra of the complexes. Usually, the experimental IR vibrational frequencies are less than the DFT-computed values. Herein, the scale factor of

0.9614 was employed to correct the DFT-calculated frequencies.[24] The NBO analysis were calculated to explore the frontier orbitals of the complexes.

The QTAIM was used to explore the nature of important bonds. The atom in molecules (AIM) calculations have been done employing the AIMALL package.[25] The QTAIM has been based on the topological analysis of the electron density, $\rho(r)$. There are several quantities of the electron density for exploring the nature of the bonds such as the kinetic energy density (G_b), the potential energy density (V_b), the total energy density (H_b), the electron density ($\rho(r)$) and its Laplacian ($\nabla^2\rho(r)$) at a bond critical point (BCP). The iso-surface Fukui maps have been computed using the Multiwfn-3.6 software.[26]

RESULTS AND DISCUSSION

Geometry optimization

The pyridoxal Schiff bases and their complexes are of great importance in biological point of view.[5,7] In this work, two vanadyl complexes of the pyridoxal Schiff bases have been newly synthesized and characterized by several experimental methods. The used Schiff bases are firstly deprotonated to produce the $\mathbf{L}^{2-}$. Then, the $\mathbf{L}^{2-}$ species is coordinated to the V(IV) metal ion. The molecular ion peaks at 423 and 471 of the mass spectra propose the [VO(A)] and [VO(B)] formula for the complexes, respectively. These formula are consistent with the CHN elemental analysis of the complexes, too (Anal. Calcd. for [VO(A)] ($C_{20}H_{24}N_4O_5V$): C, 53.22; H, 5.36; N, 12.41; V, 11.29. Found: C, 52.98; H, 5.21; N, 12.86; V, 11.61. Anal. Calcd. for [VO(B)] ($C_{22}H_{26}N_4O_5V$): C, 55.35; H, 5.49; N, 11.74; V, 10.67. Found: C, 54.87; H, 5.27; N, 11.54; V, 10.79).

Based on the proposed [VO(A)] and [VO(B)] formula for the complexes, both of the A^{2-} and B^{2-} are coordinated to the VO^{2+} in the 1:1 ratio. Firstly, the H_2A and H_2B Schiff bases are deprotonated to give the A^{2-} and B^{2-}, respectively, which act as a tetradentate ligand and are coordinated to VO^{2+} in N_2O_2 manner. This coordination manner was reported for similar tetradentate Schiff bases, previously.[5,8,18,19,27] Optimized geometries of the [VO(A)] and [VO(B)] are shown in Fig. 1, where the optimized geometries of the free H_2A and H_2B Schiff bases are given for comparison. Important structural parameters of the complexes are gathered in Table I.

Compared to the free Schiff bases, the V(IV) complexes have more planar structures. For example, the O1–O2–N4–N2 and N1–C2–C9–N3 dihedral angles are about 110 and 60° for the H_2A and H_2B Schiff bases, and about 20 and 40° for [VO(A)] and [VO(B)], respectively. Also, the N1–C2–C9 angle C5–C3–C8 are 70 and 110° for the Schiff bases, and 175 and 165° for the complexes, respectively. In the butterfly–like geometries of the free Schiff bases, two pyridine rings are in the separate planes, make a dihedral of about 40° to each other. Also, two sides of the molecule are in opposite directions. For complexation, the pyridine rings rotate around the C17–N2 and C19–N4 bonds. These rotations put the four NOON donating atoms in the same plane, provide necessary condition for coor-

dination of the Schiff base to the metal ion as a tetradentate ligand. For the free H_2A Schiff base, the calculated C1–O1–O2 and C6–N2–N4 angles are 59 and 81°, respectively,[18] which are 72 and 99° for the free H_2B,[19] respectively. These angles are 173 and 143° for [VO(A)] and 169 and 159° for [VO(B)], (Fig. 1). For comparison, the optimized geometries of the H_2A and H_2B Schiff bases are given in Fig. S-1 of the Supplementary material to this paper.

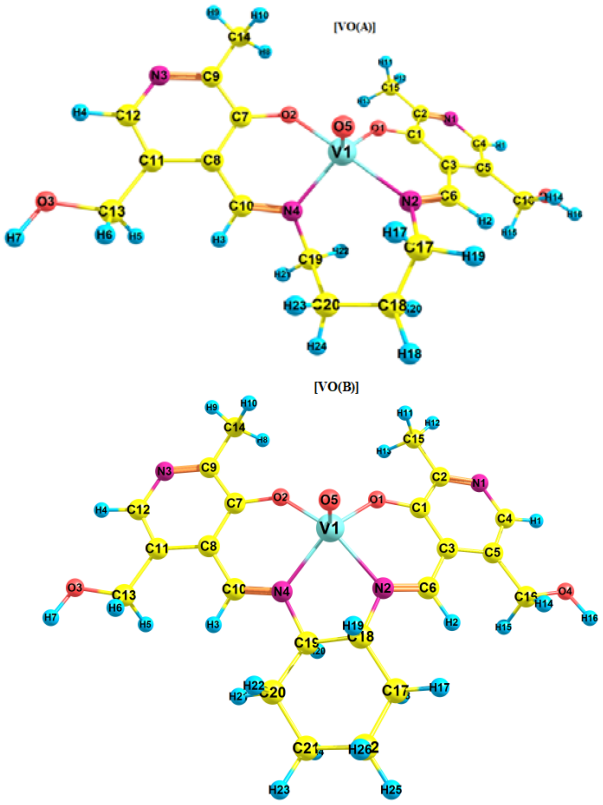

Fig. 1. Optimized geometries of [VO(A)] and [VO(B)].

Four donor atoms of the tetradentate $\mathbf{A}^{2-}$ and $\mathbf{B}^{2-}$ ligands, two deprotonated phenolate oxygens (O1 and O2 atoms) and two azomethine nitrogens (N2 and N4 atoms) lie roughly in the same plane, occupying four coordinating positions of the square base of the complexes. However, these four donating atoms and V^{4+} ion are not in the same plane (Fig. 1 and Table I), the vanadium is out of the four donating atoms. The calculated O1–O2–N4–N2 and O1–O2–N4–V dihedral angles are about 20–40°, confirming this matter. The apical position of the square–pyramidal complexes is occupied with the oxo ligand (O5). As seen in Table I, length of the V–O5 bond is significantly less than the V–O1 and V–O2 bonds.

All of the substituents as well as the azomethine groups are roughly in the same plane with the corresponding pyridine rings. The pyridine–carbon bond lengths for the $–CH_2OH$ and $–CH_3$ substitutions (about 150 pm) are proper for the pyridine-C bond (Table I). As expected, coordination of the N2 and N4 azomethine nitrogens to V^{4+} elongates the C6=N2 and C10=N4 bonds from 128 pm for the free H_2A and H_2B Schiff bases to 130 pm in the complexes. On the other hand, the Schiff bases lose their phenolic protons, which results in the C1–O1 and C7–O2 double bond. Therefore, deprotonation decreases the C1–O1 and C7–O2 bond lengths in the complexes. The calculated structural parameters are in good consistency with the corresponding values reported for the similar compounds.[2,3,5,6,8,16–19,27–30]

TABLE I. Selected structural parameters of the [VO(A)] and [VO(B)] complexes

Bond	Bond length, ppm		Angle	Angle, °		Dihedral angle	Dihedral angle, °	
	[VO(A)]	[VO(B)]		[VO(A)]	[VO(B)]		[VO(A)]	[VO(B)]
V–O1	192.6	194.0	O5–V–O1	124.0	113.6	O1–O2–N4–N2	26.4	7.3
V–O5	158.8	158.8	O5–V–N2	92.9	102.2	O1–O2–N4–V	36.0	28.00
V–N2	213.9	207.2	O1–V–O2	85.5	88.6	O5–V–O1–C1	87.9	86.2
O1–C1	130.4	130.0	O1–V–N2	84.6	85.5	O5–V–N2–C6	–118.5	–102.3
C1–C3	141.4	142.0	O1–V–N4	125.9	138.6	V–O1–C1–C3	–28.7	–22.9
C3–C6	143.8	143.6	N2–V–N4	92.8	78.7	O1–C1–C3–C6	–2.4	0.1
C6–N2	129.6	129.5	V–O1–C1	137.0	133.7	C1–C3–C6–N2	6.7	–3.2
N2–C17	147.8	147.4	O1–C1–C3	123.5	124.1	C3–C6–N2–C17	–175.7	–179.2
C17–C18	153.2	153.0	C1–C3–C6	120.5	120.7	C6–N2–C17–C18	–96.0	–6.5
C1–C2	143.4	143.7	C3–C6–N2	127.5	125.9	N2–C17–C18–C20	–70.3	179.9
C2–C15	150.1	150.1	C6–N2–C17	115.9	122.5	O1–C1–C2–C15	0.5	0.8
C2–N1	131.9	131.7	N2–C17–C18	113.8	117.6	C1–C2–N1–C4	–0.5	0.2
C5–C16	151.4	151.4	C17–C18–C20	116.6	110.3	N1–C4–C5–C16	–179.6	–179.8
C16–O4	142.2	142.2	O1–C1–C2	118.3	118.1	C4–C5–C16–O4	–3.3	–2.5
C7–O2	129.2	129.7	C1–C2–N1	121.7	121.9	C6–N2–N4–C10	–137.6	–45.4
C10–N4	130.5	129.9	C1–C2–C15	119.1	118.9	C1–O1–O2–C7	67.2	23.5
			C4–C5–C16	120.7	120.7	C5–C3–C6–N2	–175.6	177.8
			C5–C16–O4	109.8	109.9	C3–C1–C7–C9	161.0	–174.8

Vibrational spectroscopy

[VO(A)] and [VO(B)] have been identified by comparing of the experimental and DFT-calculated IR frequencies. Important vibrational frequencies of the complexes are listed in Table S-I of the Supplementary material. The C=N stretching vibration of the azomethine group results in an intensive band at 1660––1500 cm^{-1} region of the IR spectra of the Schiff bases.[2,5,6,8,18,19,27,29–35] The symmetrical stretching modes of C6=N2 and C10=N4 bonds cause an intensive band at 1628 and 1650 cm^{-1} in the IR spectra of the free H_2A and H_2B Schiff bases, respectively. Due to coordination of the N2 and N4 azomethine nitrogens to V^{4+}, electron density of the C6=N2 and C10=N4 bonds is decreased. Since,

stretching vibrations of these bonds appeared at lower energies than for the free Schiff bases, 1609 and 1633 cm^{-1} for [VO(A)] and [VO(B)], respectively.[2,5,6,8,18,19,27–29,31]

Overlapping of the O–H, N–H and C–H stretching vibration modes results in a band broading in the 3600–2000 cm^{-1} region of the IR spectra.[8,18,19,27–29,31,33–35] This region of the [VO(A)] and [VO(B)] spectra has been assigned. The obtained results are gathered in Table S-I of the Supplementary material, where the O–H stretching vibration of the $–CH_2OH$ group is the most intensive band.

In the IR spectra of the complexes, the C1–O1 and C7–O2 stretching vibrations appear at higher energies than that of the free Schiff bases. As expected, deprotonation of the phenolic oxygens increases electron density of the C1–O1 and C7–O2 bonds. The ν(C1–O1) and ν(C7–O2) vibrations of the H_2A and H_2B free Schiff bases appeared as a strong band at 1259 and 1236 cm^{-1}, respectively, and are shifted to 1390 and 1386 cm^{-1} in the IR spectra of [VO(A)] and [VO(B)], respectively.

NBO analysis

Several properties of the chemical compounds such as the atomic charges, charge transfers and molecular orbitals can be analyzed by using the NBO analysis.[19,27–29,35] Shapes of the highest occupied molecular orbital (HOMO) and the lowest unoccupied molecular orbital (LUMO) of [VO(A)] and [VO(B)] are shown in Fig. 2.

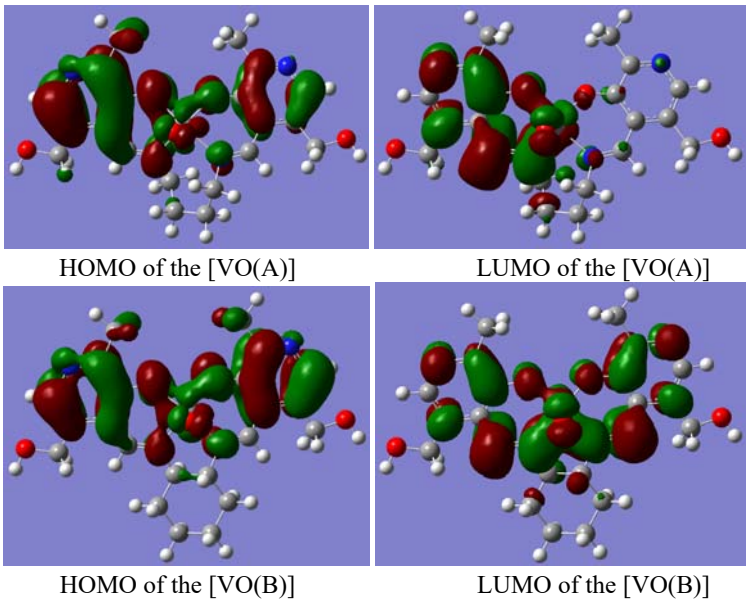

HOMO of the [VO(A)] LUMO of the [VO(A)]

HOMO of the [VO(B)] LUMO of the [VO(B)]

Fig. 2. The HOMO and LUMO frontier orbitals of the [VO(A)] and [VO(B)] complexes.

As seen in Fig. 2, both of the HOMO and LUMO orbitals of the complexes are mainly localized on the pyridine rings and the azomethine groups. The V=O5 moiety contributes mostly in the LUMO orbital of the complexes. In both of the complexes, the $–CH_3$ and $–CH_2OH$ substitutions of the pyridine rings as well as the bridge region of the complex have no role in the frontier orbitals.

The energy gap, energy difference between the HOMO and LUMO orbitals, play an important role in several properties of the chemical compounds such as the global hardness (η), photochemical reactions, electric properties and electronic spectra. Herein, the large energy gap for [VO(A)] and [VO(B)], 3.36 and 3.31 eV, respectively, confirms high stability of the complexes.[19,27–29,35,36]

QTAIM analysis

Herein, a comprehensive study of intramolecular bonds has been done employing the AIM analysis. The molecular electronic charge density ($\rho(r)$) is related to the strength of a bond. More information about the nature of the interactions is obtained from signs of the Laplacian of molecular electronic charge density ($\nabla^2\rho(r)$) and the H_b at the BCP. The molecular graphs of the investigated complexes are shown in Fig. 3. The molecular graphs of the free H_2A and H_2B Schiff bases are shown in Fig. S-2 of the Supplementary material, for the comparison.

The values of $\rho(r)$, $\nabla^2\rho(r)$, H_b, G_b, V_b and $–G_b/V_b$ at BCP are given in Table II. The hydrogen bond energies can be computed by $E_{HB} = 1/2V_b$.[37] According to Table II, the N2···H25 and N4···H26 interactions with $\nabla^2\rho(r) > 0$, $H_b < 0$, $0.5 < –G_b/V_b < 1$ and $E_{HB} = 65$ kJ mol$^{–1}$ are related to medium hydrogen bonds with partially covalent character. As seen in Fig. S-2, there are four other intramolecular H–bonds in structure of the H_2A Schiff base, all of which are the noncovalent weak interaction with $–G_b/V_b = 1.4$. Also, all of the intramolecular H-bonds in the structure of [VO(A)] and [VO(B)] are noncovalent and weak.[38]

By coordination of the azomethine nitrogens to the V(IV) metal ion, the $\rho(r)$ values of the C6=N2 and C10=N4 bonds are decreased in comparison with the corresponding free Schiff bases. This coordination results in reduction of the $\rho(r)$ in the N2–C17 and N4–C19 bonds, too. On the other hand, deprotonation and coordination of the phenolic oxygens increases the $\rho(r)$ and strength of the C1–O1 and C7–O2 bonds in comparison with the free Schiff bases. All of the V–N and V–O bonds show $0.5 < –G_b/V_b < 1$, which are classified as the partially covalent bonds. Based on the calculated $\rho(r)$ values, the V–O bonds are stronger than the V–N ones. As expected, the V–O5 is the strongest V–O bond of the complexes (Table II).

Antioxidant activity of the [VO(A)] and [VO(B)] complexes

Fig. 4 shows the DPPH radical scavenging activity of [VO(A)] and [VO(B)] in comparison with the BHA as a positive control. Both of [VO(A)] and [VO(B)]

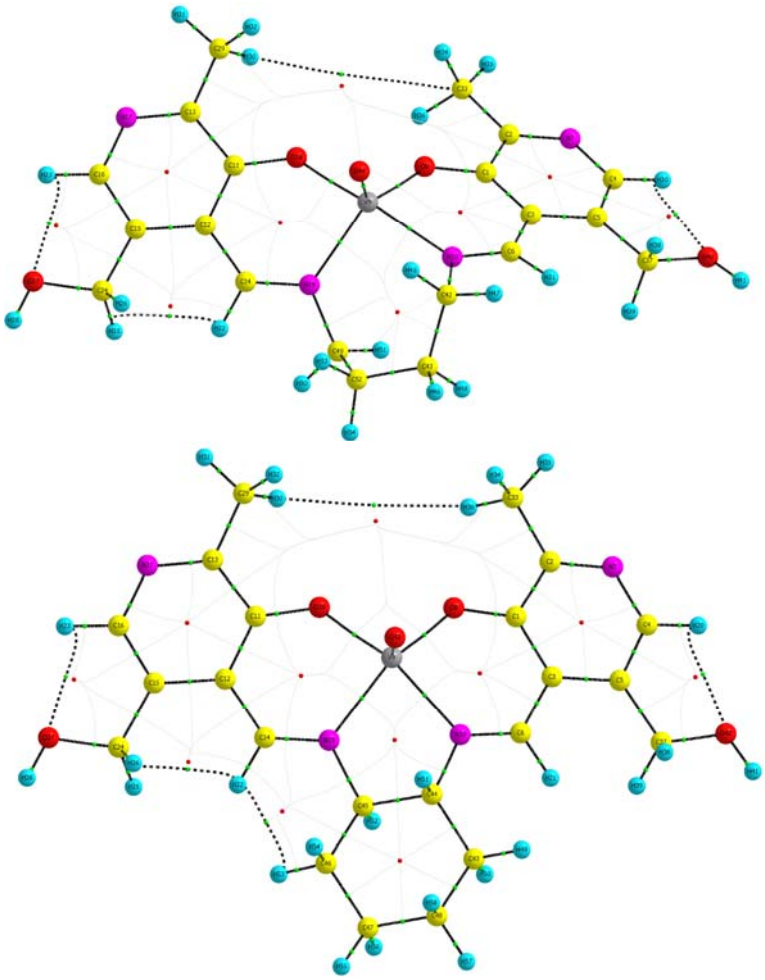

Fig. 3. QTAIM molecular graph of the [VO(A)] and [VO(B)] complexes. Small green spheres and lines correspond to the bond critical points (BCP) and the bond paths, respectively.

TABLE II. Topological parameters of the investigated species (the $\rho(r)$ in term of e/a_0^3 and all energies in term of kJ mol^{-1})

Bond	$\rho(r)$	$\nabla^2\rho(r)$	V_b	G_b	H_b	$-G_b/V_b$
			H_2A			
N2–H25	0.057565	0.124232	–120.40	100.94	–19.46	0.84
N4–H26	0.060283	0.12415	–128.00	104.71	–23.29	0.82
C6–N2	0.374767	–0.75023	–2912.45	1210.24	–1702.20	0.42
C10–N4	0.375674	–0.74304	–2927.90	1220.33	–1707.57	0.42
N2–C17	0.270023	–0.78177	–1163.12	325.23	–837.89	0.28
N4–C19	0.270023	–0.78177	–1163.12	325.23	–837.89	0.28
C1–O1	0.30463	–0.35483	–2275.77	1021.54	–1254.21	0.45
C7–O2	0.302488	–0.351	–2253.68	1011.76	–1241.91	0.45

TABLE II. Continued

Bond	$\rho(r)$	$\nabla^2\rho(r)$	V_b	G_b	H_b	$-G_b/V_b$
			H_2B			
N2–H25	0.054773	0.121636	–112.42	96.09	–16.32	0.85
N4–H26	0.057114	0.122836	–118.53	99.53	–18.99	0.84
C6–N2	0.374536	–0.76535	–2899.54	1198.83	–1700.70	0.41
C10–N4	0.37371	–0.75974	–2892.43	1197.12	–1695.32	0.41
N2–C17	0.269275	–0.77002	–1153.33	324.19	–829.13	0.28
N4–C19	0.266118	–0.74675	–1120.91	315.62	–805.31	0.28
C1–O1	0.303427	–0.36051	–2258.11	1010.85	–1247.26	0.45
C7–O2	0.30402	–0.36603	–2261.81	1010.89	–1250.91	0.45
			[VO(A)]			
H1–O4	0.015084	0.070286	–31.00	38.55	7.54	1.24
H4–O3	0.014752	0.069774	–30.40	38.08	7.67	1.25
C6–N2	0.365754	–0.66341	–2857.97	1211.46	–1646.48	0.42
C10–N4	0.359496	–0.70672	–2754.44	1145.50	–1608.92	0.42
N2–C17	0.257915	–0.71611	–1082.28	306.35	–775.94	0.28
N4–C19	0.258385	–0.71797	–1072.23	300.71	–771.50	0.28
C1–O1	0.326284	–0.13982	–2646.53	1277.42	–1369.10	0.48
C7–O2	0.337669	–0.12418	–2785.86	1352.21	–1433.65	0.49
V–N2	0.068367	0.286092	–235.41	211.52	–23.92	0.90
V–N4	0.079161	0.317339	–275.60	241.85	–33.76	0.88
V–O1	0.097748	0.550098	–407.12	383.92	–23.19	0.94
V–O2	0.090873	0.491605	–365.88	344.12	–21.74	0.94
V–O5	0.266827	1.19218	–1534.27	1158.02	–376.24	0.75
			[VO(B)]			
H1–O4	0.015065	0.070382	–30.98	38.57	7.59	1.24
H4–O3	0.015014	0.070338	–30.90	38.51	7.62	1.25
C6–N2	0.363266	–0.62488	–2850.26	1220.25	–1630.01	0.43
C10–N4	0.361806	–0.67203	–2804.09	1181.71	–1622.38	0.42
N2–C17	0.259639	–0.71279	–1084.09	308.34	–775.75	0.28
N4–C19	0.255163	–0.68048	–1009.96	281.86	–728.09	0.28
C1–O1	0.330264	–0.14344	–2690.70	1298.32	–1392.39	0.48
C7–O2	0.333728	–0.13628	–2734.32	1322.48	–1411.83	0.48
V–N2	0.081463	0.33129	–291.13	254.18	–36.93	0.87
V–N4	0.078514	0.316843	–274.89	241.33	–33.55	0.88
V–O1	0.094885	0.527674	–390.17	368.09	–22.06	0.94
V–O2	0.093547	0.515537	–383.22	360.64	–22.58	0.94
V–O5	0.266797	1.190856	–1531.46	1156.18	–375.27	0.75

showed significant DPPH radical scavenging effects in a dose-dependent manner, so the DPPH radical scavenging activity is increased at higher concentrations of the complexes. The obtained results are gathered in Table S-II of the Supplementary material. [VO(B)] had a stronger antioxidant effect than the BHA, which inhibited about 80 % of the DPPH radicals at the lowest concentration. The DPPH radical scavenging activity of [VO(A)] was close to the BHA, and the lowest concentration of this complex inhibited about 75 % of the DPPH radicals. Although both of the used Schiff base complexes showed a very strong anti-

oxidant activity during the DPPH test, [VO(B)] was a more powerful inhibitor than [VO(**A**)].

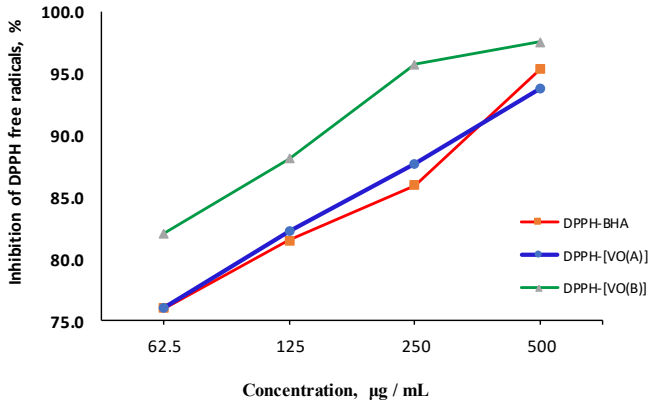

Fig. 4. The DPPH radical scavenging activity of [VO(A)] and [VO(B)] complexes in comparison with BHA.

The ABTS radical scavenging activities of the [VO(A)] and [VO(B)] complexes are shown in Fig. 5 and Table S-II together with the BHA as a positive control. Both of the complexes had a great scavenging activity against the ABTS radicals in a dose-dependent manner. Percentages of the ABTS radical scavenging at the lowest concentration of the [VO(A)] and [VO(B)] complexes were about 85 and 88 %, respectively. Similar to DPPH test, the [VO(B)] complex showed a stronger inhibitory activity than [VO(A)] complex. However, both of the Schiff base complexes had a better antioxidant activity during the ABTS test in comparison with DPPH test.

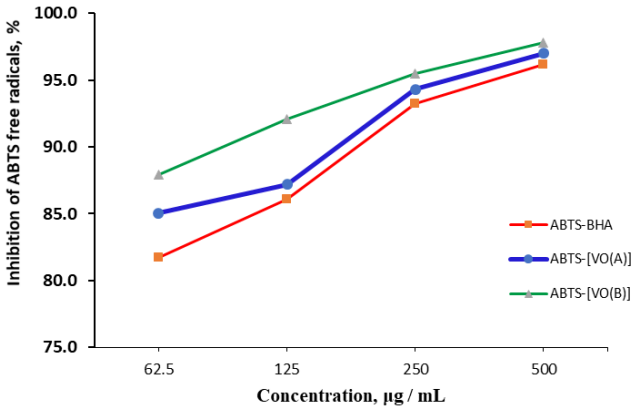

Fig. 5. The ABTS radical scavenging activity of the [VO(A)] and [VO(B)] complexes in comparison with the BHA.

The Fukui function has been widely employed in a prediction of reactive site of molecules.[39] The isosurface Fukui maps of the investigated complexes are shown in Fig. 6. As can be seen, the map is mainly on the vanadium and slightly on the phenolic oxygens since central V and two phenolic oxygens (O1 and O2 atoms) which are responsible for scavenging the radicals, have larger value of Fukui function.

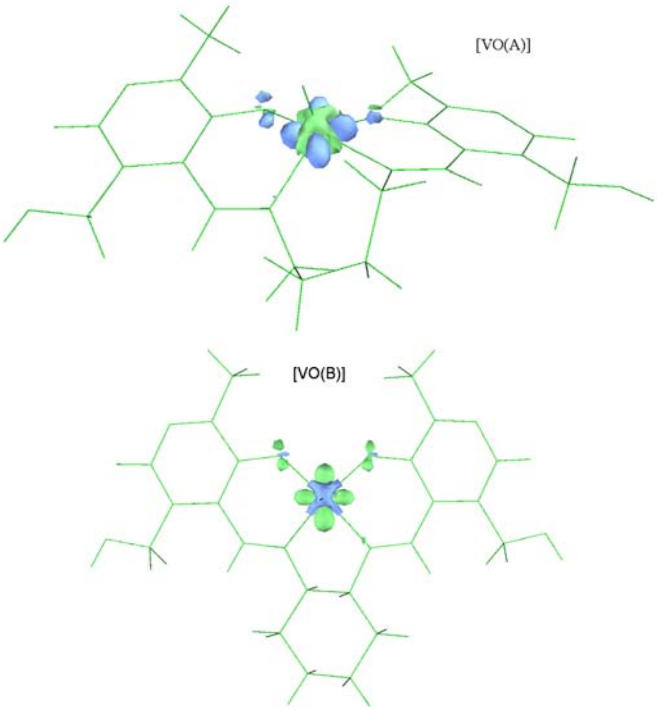

Fig. 6. The isosurface Fukui maps of the [VO(A)] and [VO(B)] complexes.

CONCLUSION

Herein, two pyridoxal Schiff bases were used to synthesize two new oxovanadium(IV) complexes. The complexes have been characterized by several experimental and theoretical methods. The H_2A and H_2B Schiff bases lose their phenolic protons, then the A^{2-} and B^{2-} moieties act as a N_2O_2 tetradentate ligand. In square pyramidal geometries of the [VO(A)] and [VO(B)] complexes, two phenolate oxygen and two azomethine nitrogen atoms of the Schiff bases occupy four coordination positions of the base. The apical position of the complexes is occupied by the oxo ligand. In the optimized geometries for the complexes, the Schiff bases have more planar structure than their free forms. The

vanadium atom is shifted upward from the square plane formed by the $\mathbf{A}^{2-}$ or $\mathbf{B}^{2-}$ ligands.

The IR vibrational frequencies of the investigated complexes have been assigned theoretically. There is good consistency between the experimental IR frequencies and the corresponding DFT–calculated values confirming suitability of the optimized geometries for the complexes. The high HOMO–LUMO energy gaps confirm stability of the complexes.

The AIM analysis shows that the C=N bonds of the azomethine groups are weaker in the complexes compared to these in the free Schiff bases. But, the C1–O1 and C7–O2 bonds of the phenolate groups are stronger for the complexes in comparison with the free Schiff bases. There are several intramolecular H-bonds in structure of the complexes, which are weak and noncovalent interactions. The $\mathbf{H_2A}$ Schiff bases involves two medium and partially covalent H-bonds.

The antioxidant properties of the synthesized complexes were examined, where the radical scavenging activities of the [VO(A)] and [VO(B)] complexes were investigated against the ABTS and DPPH radicals. Both of the complexes are more active against the ABTS radical than the DPPH one. Also, the [VO(B)] complex shows more scavenging activity than the [VO(A)] complex against both of the ABTS and DPPH radicals. It's notable that both of the used complexes show better radical scavenging activities compared to the BHA. Based on the calculated Fukui functions, the vanadium and two phenolic oxygen atoms scavenge the free radicals.

SUPPLEMENTARY MATERIAL

Optimized geometries and the QTAIM molecular graph of the H_2A and H_2B Schiff bases together with the selected experimental and theoretical IR vibrational frequencies of the [VO(A)] and [VO(B)] complexes are available electronically at the pages of journal website: http://www.shd.org.rs/JSCS/, or from the corresponding author on request.

ИЗВОД

ОКСОВАНАДИЈУМ(IV) КОМПЛЕКСИ СА ШИФОВИМ БАЗАМА ПИРИДОКСАЛА: СИНТЕЗА, ЕКСПЕРИМЕНТАЛНА И ТЕОРИЈСКА КАРАКТЕРИЗАЦИЈА, QTAIM АНАЛИЗА И АНТИОКСИДАТИВНА АКТИВНОСТ

PARISA GHORBANI[1], S. ALI BEYRAMABADI[2], MASOUD HOMAYOUNI–TABRIZI[3,*], PARICHEHREH YAGHMAEI[1]

[1]*Department of Biology, Science and Research Branch, Islamic Azad University, Tehran, Iran;*
[2]*Department of Chemistry, Mashhad Branch, Islamic Azad University, Mashhad, Iran;*
[3]*Department of Biology, Mashhad Branch, Islamic Azad University, Mashhad, Iran*

Описана је синтеза и спектроскопска карактеризација два нова оксованадијум(IV) комплекса са Шифовим базама пиридоксала (H_2L), 4,4′-[1,4-бутандиилбис-[(*E*)-нитрилометилидин])бис[5-хидрокси-6-метил-3-пиридинметанол] и *trans*-4,4′-[1,2-циклохексилбис-[(*E*)-нитрилометилидин])бис[5-хидрокси-6-метил-3-пиридинметанол]. Оптимизација геометрије, одређивање инфра–црвених вибрационих фреквенција и анализа природних везивних орбитала (NBO) комплекса урађени су коришћењем метода базираних на теорији функционала густине. Депротонована форма Шифових база (L^{2-}) се као тетрадентатни N_2O_2 лиганд координује за V(IV) јон преко два фенолатна кисео-

никова атома и два иминска атома азота. У апикалном положају квадратно–пирамидалне геометрије [VO(L)] комплекса налази се оксо–лиганд. DFT израчунавања вибрационих фреквенција су у доброј сагласности са одговарајућим експерименталним вредностима чиме је потврђена добра оптимизација геометрије комплекса. Природа и врсте везивних интеракција су одређене применом квантне атомске теорије (QTAIM) анализе молекула. Услед формирања комплекса долази до слабљења јачине C–N везе из азометинске групе и јачања C–O везе фенолатних група. Високоенергетски скок потврђује стабилност комплекса. Оба комплекса су показала значајну антиоксидативну активност.

(Примљено 29. јануара, ревидирано 14. априла, прихваћено 24. маја 2019)

REFERENCES

1. S. Saha, A. Das, K. Acharjee, B. Sinha, *J. Serb. Chem. Soc.* **81** (2016) 9 (http://doi.org/10.2298/jsc160425065s)
2. E. G. Bakirdere, M. F. Fellah, E. Canpolat, M. Kaya, S. Gür, *J. Serb. Chem. Soc.* **81** (2016) 12 (http://doi.org/10.2298/jsc151030008b)
3. H. Amiri Rudbari, M. R. Iravani, V. Moazam, B. Askari, M. Khorshidifard, N. Habibi, G. Bruno, *J. Mol. Struct.* **1125** (2016) 113 (https://doi.org/10.1016/j.molstruc.2016.06.055)
4. M. S. S. Adam, H. Elsawy, *J. Photochem. Photobiol., B* **184** (2018) 34 (https://doi.org/10.1016/j.jphotobiol.2018.05.002)
5. T. Mukherjee, J. O. Costa Pessoa, A. Kumar, A. R. Sarkar, *Inorg. Chem.* **50** (2011) 4349 (http://doi.org/10.1021/ic102412s)
6. M. Sankarganesh, N. Revathi, J. D. Raja, K. Sakthikumar, G. G. Vinoth Kumar, J. Rajesh, M. Rajalakshmi, L. Mitu, *J. Serb. Chem. Soc.* **84** (2018) 277 (http://doi.org/10.2298/jsc180609080s)
7. S. Yadamani, A. Neamati, M. Homayouni–Tabrizi, S. A. Beyramabadi, S. Yadamani, A. Gharib, A. Morsali, M. Khashi, *The Breast* **41** (2018) 107 (https://doi.org/10.1016/j.breast.2018.07.001)
8. F. Jafari–Moghaddam, S. A. Beyramabadi, M. Khashi, A. Morsali, *J. Mol. Struct.* **1153** (2018) 149 (https://doi.org/10.1016/j.molstruc.2017.10.007)
9. S. Menati, H. A. Rudbari, M. Khorshidifard, F. Jalilian, *J. Mol. Struct.* **1103** (2016) 94 (https://doi.org/10.1016/j.molstruc.2015.08.060)
10. D. Sanna, V. Ugone, M. Serra, E. Garribba, *J. Inorg. Biochem.* **173** (2017) 52 (https://doi.org/10.1016/j.jinorgbio.2017.04.023)
11. J. Berg, JL; Stryer, L., Biochemistry, in, WH Freeman and Company: New York, 2002,
12. P. P. Cohen, *Biochem. J.* **33** (1939) 1478 (PMCID: PMC1264599)
13. R.–Ş. Mezey, I. Máthé, S. Shova, M.–N. Grecu, T. Roşu, *Polyhedron* **102** (2015) 684 (https://doi.org/10.1016/j.poly.2015.10.035)
14. R. Manikandan, P. Vijayan, P. Anitha, G. Prakash, P. Viswanathamurthi, R. J. Butcher, K. Velmurugan, R. Nandhakumar, *Inorg. Chim. Acta* **421** (2014) 80 (https://doi.org/10.1016/j.ica.2014.05.035)
15. B. Annaraj, M. A. Neelakantan, *Eur. J. Med. Chem.* **102** (2015) 1 (https://doi.org/10.1016/j.ejmech.2015.07.041)
16. S. A. Elsayed, A. M. Noufal, A. M. El–Hendawy, *J. Mol. Struct.* **1144** (2017) 120 (https://doi.org/10.1016/j.molstruc.2017.05.020)
17. T. Rosu, E. Pahontu, M. Reka–Stefana, D.–C. Ilies, R. Georgescu, S. Shova, A. Gulea, *Polyhedron* **31** (2012) 352 (https://doi.org/10.1016/j.poly.2011.09.044)

18. H. Eshtiagh–Hosseini, M. R. Housaindokht, S. A. Beyramabadi, S. H. M. Tabatabaei, A. A. Esmaeili, M. J. Khoshkholgh, *Spectrochim. Acta, Part A* **78** (2011) 1046 (https://doi.org/10.1016/j.saa.2010.12.045)
19. S. Beyramabadi, A. Morsali, A. Shams, *J. Struct. Chem.* **56** (2015) 243 (https://doi.org/10.1134/S0022476615020067)
20. C. Lee, W. Yang, R. G. Parr, *Phys. Rev. B: Condens. Matter Mater. Phys.* **37** (1988) 785 (http://doi.org/10.1103/PhysRevB.37.785)
21. M. Frisch, G. Trucks, H. Schlegel, G. Scuseria, M. Robb, J. Cheeseman, J. Montgomery Jr, T. Vreven, K. Kudin, J. Burant, *Inc., Pittsburgh, PA* (2003) 12478
22. P. J. Hay, W. R. Wadt, *J. Chem. Phys.* **82** (1985) 270 (https://doi.org/10.1063/1.448799)
23. https://www.chemcraftprog.com (last accessed 12 Feb, 2020)
24. D. C. Young, Computational Chemistry: A Practical Guide for Applying Techniques to Real World Problems, Wiley Online Library, New York, 2001
25. T. A. Keith, TK Gristmill Software, Overland Park KS, USA (2013)
26. T. Lu, F. Chen, *J. Comput. Chem.* **33** (2012) 580 (https://doi.org/10.1002/jcc.22885)
27. T. Toozandejani, S. A. Beyramabadi, H. Chegini, M. Khashi, A. Morsali, M. Pordel, *J. Mol. Struct.* **1127** (2017) 15 (https://doi.org/10.1016/j.molstruc.2016.07.026)
28. H. Eshtiagh–Hosseini, M. R. Housaindokht, S. A. Beyramabadi, S. Beheshti, A. A. Esmaeili, M. J. Khoshkholgh, A. Morsali, *Spectrochim. Acta, Part A* **71** (2008) 1341 (https://doi.org/10.1016/j.saa.2008.04.019)
29. S. A. Beyramabadi, A. Morsali, M. J. Khoshkholgh, A. A. Esmaeili, *Spectrochim. Acta, Part A* **83** (2011) 467 (https://doi.org/10.1016/j.saa.2011.08.067)
30. N. V. Tverdova, E. D. Pelevina, N. I. Giricheva, G. V. Girichev, N. P. Kuzmina, O. V. Kotova, *J. Mol. Struct.* **1012** (2012) 151 (https://doi.org/10.1016/j.molstruc.2011.06.037)
31. C. Kanagavalli, M. Sankarganesh, J. Dhaveethu Raja, M. Kalanithi, *J. Serb. Chem. Soc.* **84** (2018) 267 (https://doi.org/10.2298/jsc180521101k)
32. M. Ben Gzaiel, A. Oueslati, I. Chaabane, M. Gargouri, *J. Mol. Struct.* **1122** (2016) 280 (https://doi.org/10.1016/j.molstruc.2016.05.097)
33. Z. Moosavi–Tekyeh, N. Dastani, *J. Mol. Struct.* **1102** (2015) 314 (https://doi.org/10.1016/j.molstruc.2015.09.001)
34. G. Mariappan, N. Sundaraganesan, *J. Mol. Struct.* **1074** (2014) 51 (https://doi.org/10.1016/j.molstruc.2014.04.022)
35. R. Mathammal, K. Sangeetha, M. Sangeetha, R. Mekala, S. Gadheeja, *J. Mol. Struct.* **1120** (2016) 1 (https://doi.org/10.1016/j.molstruc.2016.05.008)
36. A. Kanaani, D. Ajloo, G. Grivani, A. Ghavami, M. Vakili, *J. Mol. Struct.* **1112** (2016) 87 (https://doi.org/10.1016/j.molstruc.2016.02.024)
37. E. Espinosa, M. Souhassou, H. Lachekar, C. Lecomte, *Acta Crystallogr., Sect. B: Struct. Sci.* **55** (1999) 563 (https://doi.org/10.1107/S0108768199002128)
38. I. Rozas, I. Alkorta, J. Elguero, *J. Am. Chem. Soc.* **122** (2000) 11154 (https://doi.org/10.1021/ja0017864)
39. R. G. Parr, W. Yang, *J. Am. Chem. Soc.* **106** (1984) 4049 (https://doi.org/10.1021/ja00326a036).